國立交通大學

電子物理研究所

碩士論文

碲硒化鋅磊晶層中的碲等電性中心之光激螢光時間解析光譜

Time-resolved photoluminescence of Te isoelectronic centers in ZnSe$_{1-x}$Te$_x$ epilayers

研 究 生：柯復凱

指導教授：周武清　教授

中華民國九十七年六月

碲硒化鋅磊晶層中的碲等電性中心之光激螢光時間解析光譜

Time-resolved photoluminescence of Te isoelectronic centers in $ZnSe_{1-x}Te_x$ epilayers

研究生：柯復凱　　**Student：Fu-Kai Ke**

指導教授：周武清 教授　　**Advisor：Prof. Wu-Ching Chou**

國立交通大學
電子物理研究所
碩士論文

A Thesis
Submitted to Institute of Electrophysics
College of Science
National Chiao Tung University
in partial Fulfillment of the Requirements
for the Degree of Master
in
Electrophysics
June 2008
Hsinchu, Taiwan, Republic of China

中華民國九十七年六月

碲硒化鋅磊晶層中的碲等電性中心之光激螢光時間解析光譜

研究生：柯復凱　　　　　　　　指導教授：周武清 博士

國立交通大學電子物理研究所

中文摘要

我們使用光激螢光譜和時間解析光譜來分析參雜不同碲濃度的碲硒化鋅磊晶層(碲莫耳濃度小於百分之四十二)。我們發現不同碲濃度的碲硒化鋅複合時間在數個奈秒到數十個奈秒之間。當碲莫耳濃度由零增加到百分之十時，最長的複合時間到達七十八奈秒。複合時間的增加是由於局部位能隨碲濃度增加而變大。當碲濃度再度增加，複合時間卻隨著碲濃度的增加而減少。這現象可以被碲的局部態和主要的價帶混成的模型解釋。藉著不同碲濃度之激子束縛能、光激螢光譜的半高寬和熱活化能的結果都支持這驅勢。

Time-resolved photoluminescence of Te isoelectronic centers in $ZnSe_{1-x}Te_x$ epilayers

Student：Fu-Kai Ke **Advisor：Dr. Wu-Ching Chou**

Institute of Electrophysics
National Chiao Tung University

Abstract

$ZnSe_{1-x}Te_x$ ($x \leqq 0.42$) epilayers grown by molecular beam epitaxy were studied by photoluminescence (PL) and time-resolved photoluminescence (TRPL). The recombination time varies with Te concentration from a few nanoseconds to tens of nanosecond. The recombination time reaches a maximum value of about 78 ns when x increases from 0 to 0.10. The increase of the recombination time is attributed to the increasing localization potential with Te concentration. As the Te composition is further increased, the exciton recombination lifetime decreases with x. This behavior can be explained by the hybridization of Te localized states and the host valence band states. This tendency can be further supported by the dependence of the PL line width, exciton binding energy, and thermal activation energy on the Te concentration.

Acknowledgement

兩年的碩士生涯即將結束，我學會了思考問題與克服壓力，用心思考每一個問題，通常問題都能找到較好的辦法解決。當然也要感謝交大土地公幫了我很多忙，對於在學校有任何不能解決的問題我總是不厭其煩的去拜拜，謝謝土地公的保佑。這兩年讓我體會到要學習的事物實在太多了，但唯有從學習中才會能更了解自己的不足。

這篇碩士論文能夠完成，我由衷的感謝指導教授周武清老師的支持與教導，提供我良好的實驗環境研究，也常常給我中肯而且相當關鍵的建議，不論在學術研究或待人處事上我都受益許多；也特別感謝李明知老師、陳衛國老師及張文豪老師，以及徐子民老師能即時地給我許多研究上的寶貴意見，讓我了解到人外有人、學海無涯的道理。同時，我也要謝謝這一年多來帶領我的游泳教練兼學長彥丞，因為經驗豐富的學長總能給我許多自己想不到的建議，這才讓我能夠有更加順利的研究進度。

對於實驗室的學長姐：繼祖、瑞雯、彥丞、怡仁、狗哥、龜泰、崑峰等，謝謝你們的能夠分享自己的研究經驗以及給我指導與鼓勵，使我能順利畢業，希望跟我同年畢業的繼祖學長未來能夠在中研院一樣有傑出的研究成果，也祝福其他學長姐和正要去光電所唸博班的鏡學都能早點順利畢業。還有我的室友阿吉學長以及兩位優秀的學弟俊榮、威智，有你們的陪伴，讓我的碩士生涯更加有樂趣。祝福阿吉目前就任的公司未來能夠大發利市，兩學弟順利畢業。當然不能忘記感謝目前在台積電工作的筱筑學姊，妳的能幹體貼，讓我和鏡學備受感動，希望妳未來能夠有好的婚姻。

最後還是要感謝輔仁大學物理系的林更清老師以及劉建楠老師，有你們的推薦函，我才有機會體會到這間風格完全異於輔大的學校。更重要的是我的父母和家人支持我念完碩士，讓我這一生的有更多機會去體驗不同階段的學生生活。

Index

Chapter 1：Introduction

In recent years, isoelectronic centers (ICs) in semiconductors have attracted much interest due to their distinct physical properties from normal semiconductors. Semiconductor with IC is formed by partially replacing a host atom by another atom with the same number of valance electrons. Because the replaced atoms are of different electro-negativity from the original atoms, electrons or holes (depends on the content of replaced atoms) can be localized in such IC trap states [1]. It was shown in recent studies on GaNP and GaNAs, the interaction between N isoelectronic traps and the conduction band edge of GaP and GaAs has a great effect on their band structures [2]. In II-VI compound semiconductors, the effect of IC were also studied in ZnTeO [3] and ZnSTe [4]. However, the recombination dynamics of ZnSeTe has not been studied in detail, despite this compound semiconductor has been realized as high-brightness blue and green light-emitting diodes [5]. The difference in electro-negativity between Te and Se atoms results in the isoelectronic Te-bound excitons and affects the optical properties of ZnSeTe [1, 6]. Furthermore, the decay dynamics of Te-bound excitons in $ZnSe_{1-x}Te_x$ ternary alloys are very important to understand the emission mechanism of the bright light emitting devices. In comparison with binary compound semiconductor ZnSe, the luminescence decay rates are two orders of magnitude smaller than that of ZnSeTe. For example, Fu *et al.*, [7] Reznitsky *et al.*, [8] and Gu *et al.*, [9] respectively found that the decay time of 20, 38, and 30 ns for $ZnSe_{1-x}Te_x$ of $x = 0.010$, 0.018, and 0.120. However, the dependence of decay time on the Te composition of $ZnSe_{1-x}Te_x$ remains unexplored.

In chapter 2, the sample preparations using Veeco Applied EPI 620 molecular-beam epitaxy (MBE) system are introduced. In addition, the photoluminescence (PL) and time-resolved PL (TRPL) measurements are decided. In chapter 3, the results of PL and TRPL measurements will be discussed. Finally, a brief conclusion of current work is given in chapter 4.

Chapter 2: Experiment

In this chapter, the growth of $ZnSe_{1-x}Te_x$ ($0.005 \leqq x \leqq 0.42$) samples and the experimental techniques used in this thesis were described. The experimental techniques include photoluminescence (PL), and time-resolved PL (TRPL).

2.1 Sample preparation

The $ZnSe_{1-x}Te_x$ ($0.005 \leqq x \leqq 0.42$) epilayers were grown on GaAs (001) substrates by the EPI 620 molecular beam epitaxy (MBE) as shown in Fig. 2-1. EPI 40 cc low temperature cells were used for evaporation of the elemental solid sources: Zn, Se, and Te. The cell temperatures of Zn were fixed at 300 °C. The cell temperatures of Se were set between 178 °C and 162 °C. The cell temperatures of Te were between 230 °C and 310 °C. The temperature of substrate was fixed at 300 °C. During the growth, reflected high-energy electron diffraction (RHEED) was used to moniator the process of epitaxial growth. The Te concentration was determined by energy dispersive x-ray (EDX) measurements.

2.2 Photoluminescence (PL) system

The schematic setup of the photoluminescence system is shown in Fig. 2-2. The samples were loaded on the cold finger of a closed cycle cryostat. The temperature can be controlled between 10 and 325 K. The sample was excited by a GaN pulsed laser (405 nm) with a pulse width of 50 ps and a repetition rate of 2.5 MHz. The incident laser beam is focused on the sample by a convex lens (L_1). The combination of a set of convex lenses (L_2 and L_3) guide the luminescence into the double-grating spectrometer. A SPEX 1403 double-grating spectrometer equipped with a thermoelectrically cooled photo-multiplier tube (PMT; R928, Hamamatsu) is used to detect the PL spectra. The spectrometer is controlled by a computer which is used to store and plot the collected data.

2.3 Time-resolved photoluminescence (TRPL) system

The setup of TRPL system is shown in Fig. 2-3. The GaN pulsed laser (405 nm) with a pulse width of 50 ps and a repetition rate of 2.5 MHz was used as an excitation source. The laser light was focused on the sample by a convex lens (L_1). The combination (L_2 and L_3) lenses guides the luminescence into the double-grating spectrometer. The signal is dispersed by a 0.85 m double-grating spectrometer and detected by a high-speed photomultiplier tube. The singles were further analyzed by a computer plug-in time-correlated counting card. The overall temporal resolution of the TRPL measurement is about 300 ps.

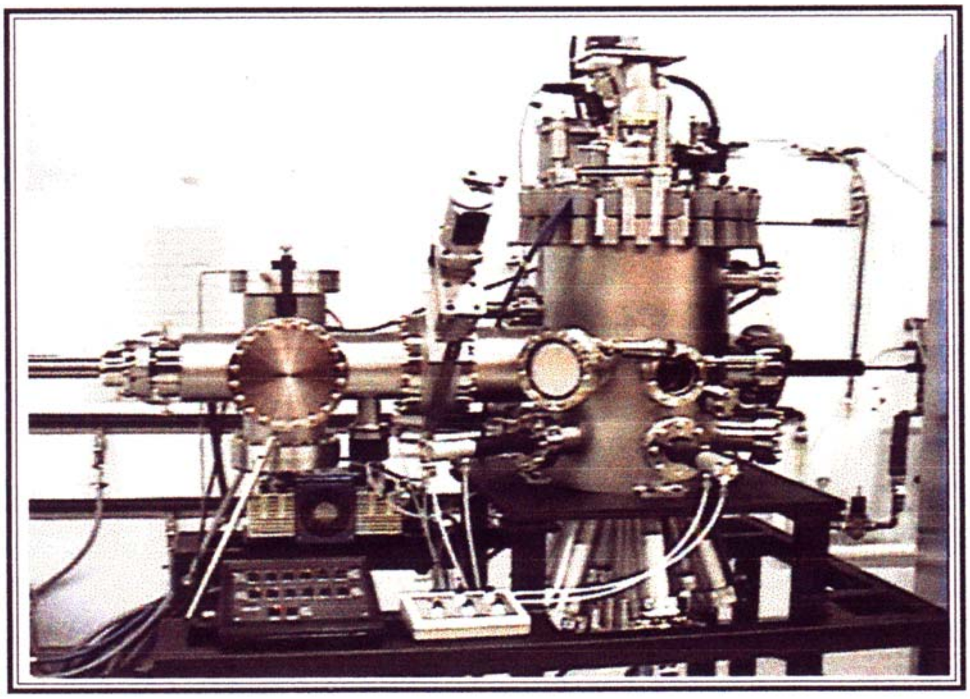

Fig 2-1. Veeco Applied EPI 620 molecular beam epitaxy (MBE) system.

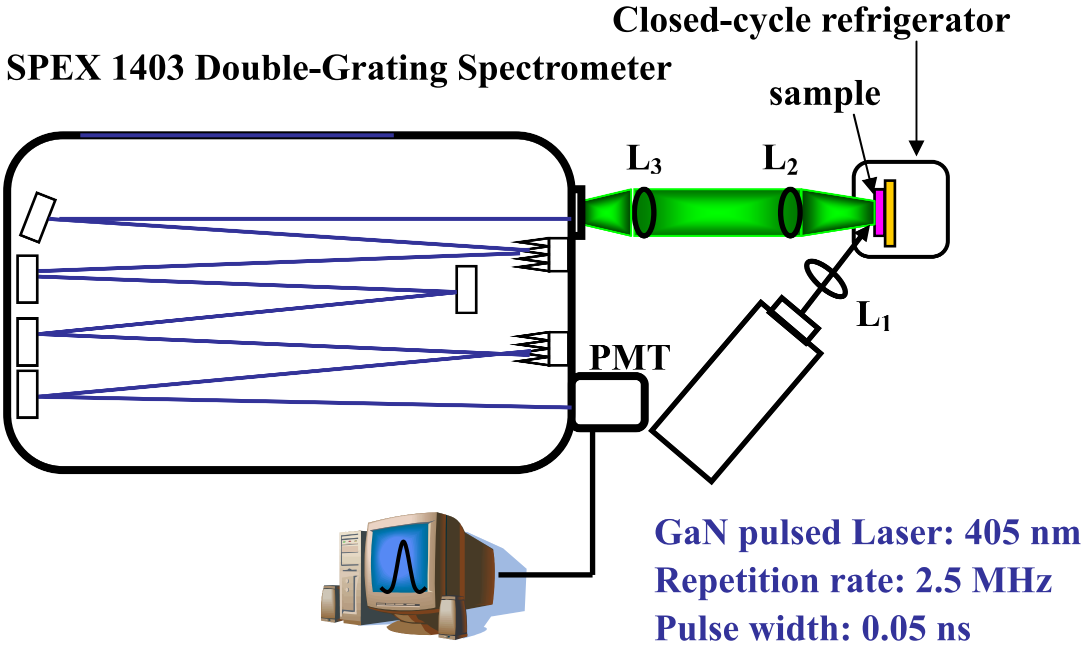

Fig. 2-2. The experimental setup of the PL measurements.

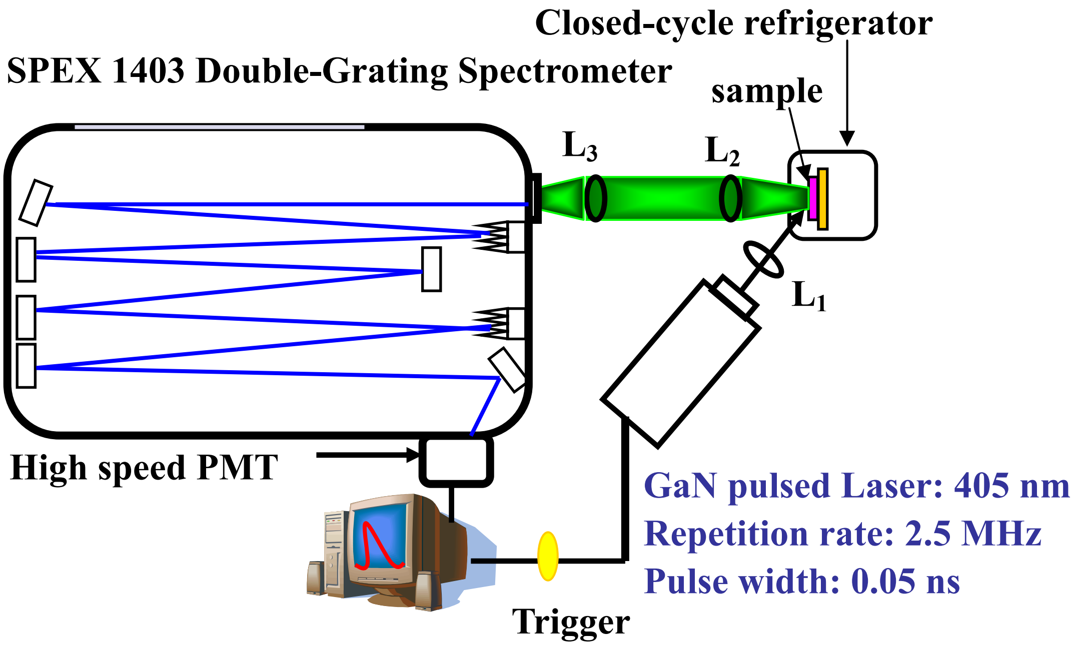

Fig. 2-3. The experimental setup of the TRPL measurements.

Chapter 3: Results and Discussion

In this chapter, we study the recombination kinetics of $ZnSe_{1-x}Te_x$ ternary alloys with wide Te composition ranges from 0.005 to 0.420 by PL and TRPL measurements. The results are described below.

3.1 Photoluminescence study of $ZnSe_{1-x}Te_x$

The normalized PL spectra of $ZnSe_{1-x}Te_x$ ($0.005 \leqq x \leqq 0.42$) at 13 K are shown in Fig. 3-1. It is obvious that the main peak of PL emission shifts to lower energies with the increasing of x, from 2.66 to 2.17 eV for x = 0.005 and 0.42, respectively. These PL emissions have generally been attributed to excitons bound to isoelectronic Te_{Se} (atoms and/or clusters) in ZnSe [6]. As shown in Fig 3-1, the PL peak at 2.78 eV for the x = 0.005 sample is attributed to excitons localized at a single Te atom (Te_1) [1]. A peak at around 2.66 eV is attributed to the Te_2 complexes [6], which dominates the PL spectrum for x = 0.005 sample. When the Te concentration is further increased, the PL emissions evolve from the Te_2 complexes to the exction bound to Te_n ($n \geqq 3$) clusters [6]. The origins of different PL emissions are indicated by dashed lines in Fig. 3-1.

Fig. 3-2 shows the exciton binding energy as a function of Te composition. The energy difference between the band gap of $ZnSe_{1-x}Te_x$ alloy and the measured PL peak energy is defined as the exciton binding energy (denoted as E_b) [10]. The band gap of $ZnSe_{1-x}Te_x$ can be written as

$$E_g(x) = 1.57x^2 - 1.953x + 2.82, \qquad (1)$$

which is fitted by *Brasil et al.*[11] from their optical results, as plotted in Fig. 3-3 with our PL peak energy data. From Fig. 3-2, it can be seen that binding energy increases as the Te concentration increases. The binding energy reaches a maximum of about 272 meV when Te is increased from 0 to 10 %. However, when Te composition is further increased, the binding energy decreases monotonically. This is because the exciton localization of Te isoelectronic centers is closely related to the size of the Te_n clusters. The larger Te_n clusters have higher binding energy. Nevertheless, when the Te_n clusters become to large enough, the difference between the isoelectronic potential and the host atomic potential will be reduced.

Fig. 3-4 shows the measured PL line-width as a function of Te composition. The composition dependence of the line width has a similar tendency to the dependence of exciton binding energy on Te concentration. The full width at half maximum (FWHM) of the PL spectra increases from 120 to 160 meV as x increases from 0.005 to 0.060. As the Te concentration is further increased, monotonously drop of the FWHM can be observed. The huge line-width broadening cannot be totally ascribed to Te compositional fluctuation because the line-width broadening of non-isoelectronic ternary semiconductors is only 16 ~ 39 meV in $Zn_{1-x}Mg_xTe$ ($0.10 \leqq x \leqq 0.52$), 10 ~ 40 meV in $Zn_{1-x}Mn_xTe$ ($0.10 \leqq x \leqq 0.56$) [12] and 10 ~ 50 meV in $Al_xGa_{1-x}N$ ($0 \leqq x \leqq 0.50$) [13].

Due to the fact that a strong localization is accompanied by isoelectronic centers and results in the increase of the line-width of the photon emission. However, it is difficult to specify the line-width of one specific isoelectronic center, because more than one Te_n centers are involved in the PL spectrum in most samples. Nevertheless, for the samples with small Te composition (x = 0.005 – 0.060), the dominated PL peaks roughly correspond to the Te_2 complexes and Te_n clusters. Therefore, it is reasonable to assume that the line-width increases as the Te impurity evolves from Te_2 complexes to Te_n clusters.

The temperature dependence of the integrated PL intensity (I_{PL}) can be expressed as

$$I_{PL}(T) = \frac{I_0}{1 + A\exp(-E_a / k_B T)}, \qquad (2)$$

where T is the temperature, k_B is the Boltzmann constant, I_0 is the integrated PL intensity at 0 K, A is a constant, and E_a is the thermal activation energy [14 - 16].

E_a is responsible for the thermal quenching of PL intensity in the temperature-dependent PL spectra. The PL intensity versus temperature of $ZnSe_{0.94}Te_{0.06}$ epilayer is shown in Fig. 3-5. The thermal activation energy of $ZnSe_{0.94}Te_{0.06}$ epilayer can be fitted using equation 2 as shown in Fig. 3-5.

Figure 3-6 presents the thermal activation energies E_a as a function of Te composition of all the $ZnSe_xTe_{1-x}$ samples. As the Te concentration of the $ZnSe_xTe_{1-x}$ alloys increases from 0.005 to 0.100, E_a increases initially from 88 to 130 meV. If the Te concentration is further increased, the thermal activation energy decreases monotonously. The temperature-induced quenching of luminescence in the epilayers mainly attributes to the thermal dissociation of excitons into free electrons and holes [16].

3.2 Time-resolved photoluminescence study of $ZnSe_{1-x}Te_x$

In order to understand the recombination mechanism of $ZnSe_{1-x}Te_x$, the TRPL measurements were performed. The PL decay times were focused on the peak position of each PL spectrum. At low temperature, the PL is dominated by the radiative recombination and the nonradiative recombination could be neglected. Therefore, the measured decay time can be regarded as the radiative recombination lifetime of the bound excitons. The PL decay profiles were plotted in the logarithmic scale, shown in Fig. 3-7. As the Te content increases from 0.5 to 10 %, the PL decay lifetime increases. However, when Te composition is further increased, the PL decay lifetime decreases monotonically. Additionally, the decay profiles are clearly non-single exponential decay. It could be due to different emission origins from various isoelectronic centers, which results in multiple exponential PL decay. Therefore, all the TRPL spectra can be fitted by using stretched exponential

$$\mathrm{I(t)} = \mathrm{I}_0 \exp\left[-\left(\frac{t}{\tau}\right)^{\beta}\right], \qquad (3)$$

where β is the stretching parameter, and I(t) is the PL intensity as a function of time [17 – 25]. Stretched exponentials have been used to describe the localized states that act as traps and cause a distribution of trap energies [17]. The stretched exponential fitting method was first used by Chen *et al.*[18] for disordered semiconductors. Figure 3-8 presents the PL decay curves in a double logarithmic scale and fitted by stretched exponential function.

The PL decay lifetimes as a function of Te concentration are shown in Fig. 3-9. The recombination lifetime varies from a few nanoseconds to tens of nanoseconds with different Te concentration. When x is small ($x < 0.100$), the lifetime increases with x. As the Te content increases, the recombination lifetime increases and reaches a maximum at about 78 ns for $x = 0.10$. This implies that when the Te isoelectronic centers gradually evolve from Te_2 complexes to Te_n clusters, the corresponding radiative recombination lifetime increases. The Te_n clusters have deeper localized short-range potentials and thus result in a larger binding energy. Therefore, the bound exciton states are more localized in the real space, leading to the reduced electronic - hole overlap for the self - trapped excitons and excitons localized at one center tunnel over barrier to another center. As a result, the radiative recombination lifetime increase [7, 26, 27]. When $x > 0.100$, however, the PL decay times are found to decrease with further increase of x. It is due to the fact that when the Te_n clusters become large enough, the bound exciton states decrease (such as FWHM). Thus, the difference between the different localize states will be diminishing resulting in the formation of the hybridized states and towards the band state of ZnTe. The decrease of recombination lifetime with x reflects the decreasing percentage of excitons that tunnel between different localize states [7, 28]. For x close to 0.420, the delocalized nature of the host band states leads to the observed short recombination lifetime.

Figure 3-10 shows the PL decay time as a function of the monitored emission energies for the three samples. The general trend is that when the monitored energy decreases, the measured decay time increases. This result is consistent with the fact that the lower energy position corresponds to larger Te_n clusters [1]. For example, for the sample of x=0.005, the high energy side of the PL contain the contribution of Te_1, the central part of the PL is dominated by Te_2 complexes, and the lower energy side comprises the PL contribution of Te_n clusters.

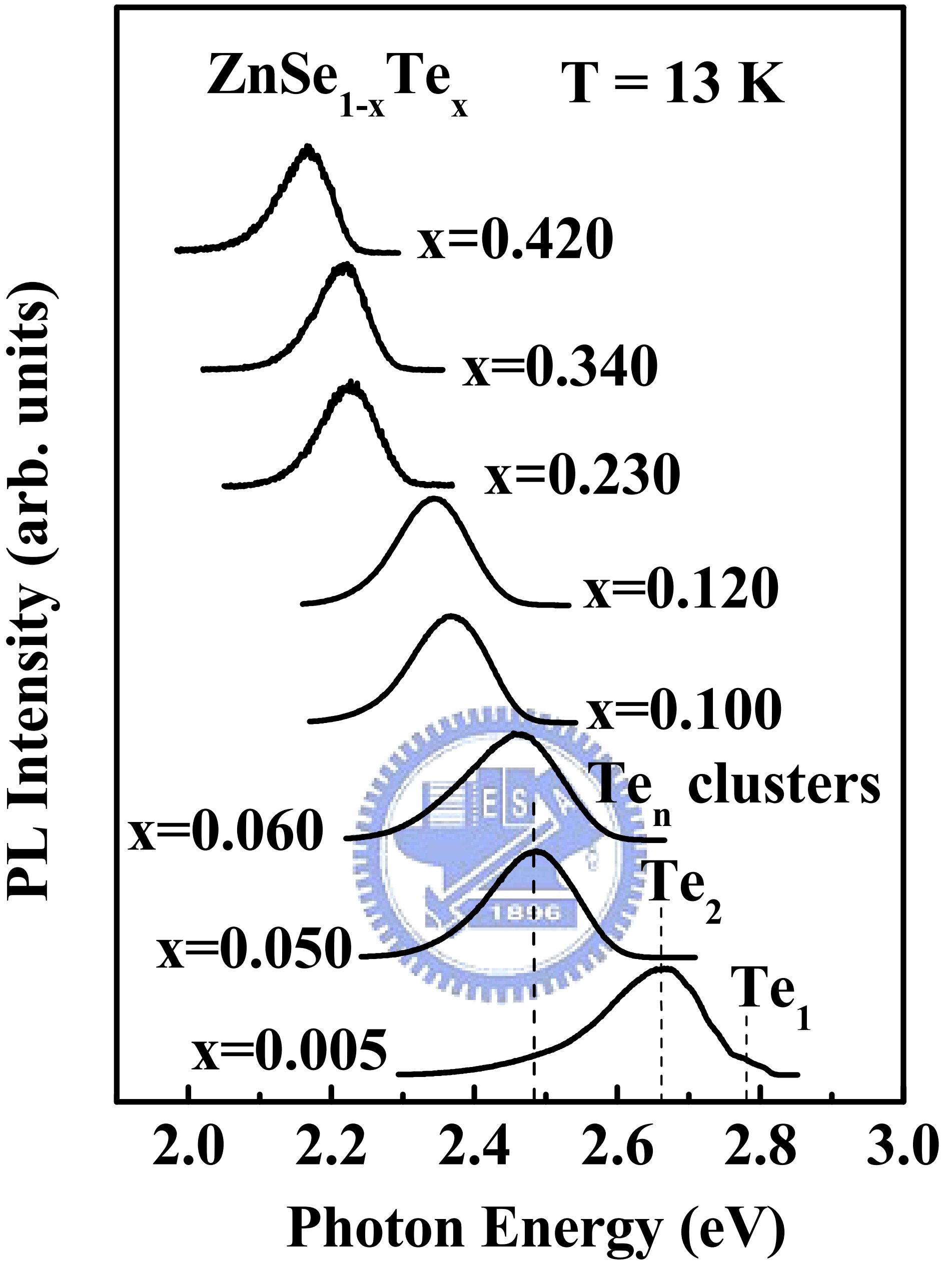

FIG. 3-1. Normalized PL spectra of $ZnSe_{1-x}Te_x$ at 13 K.

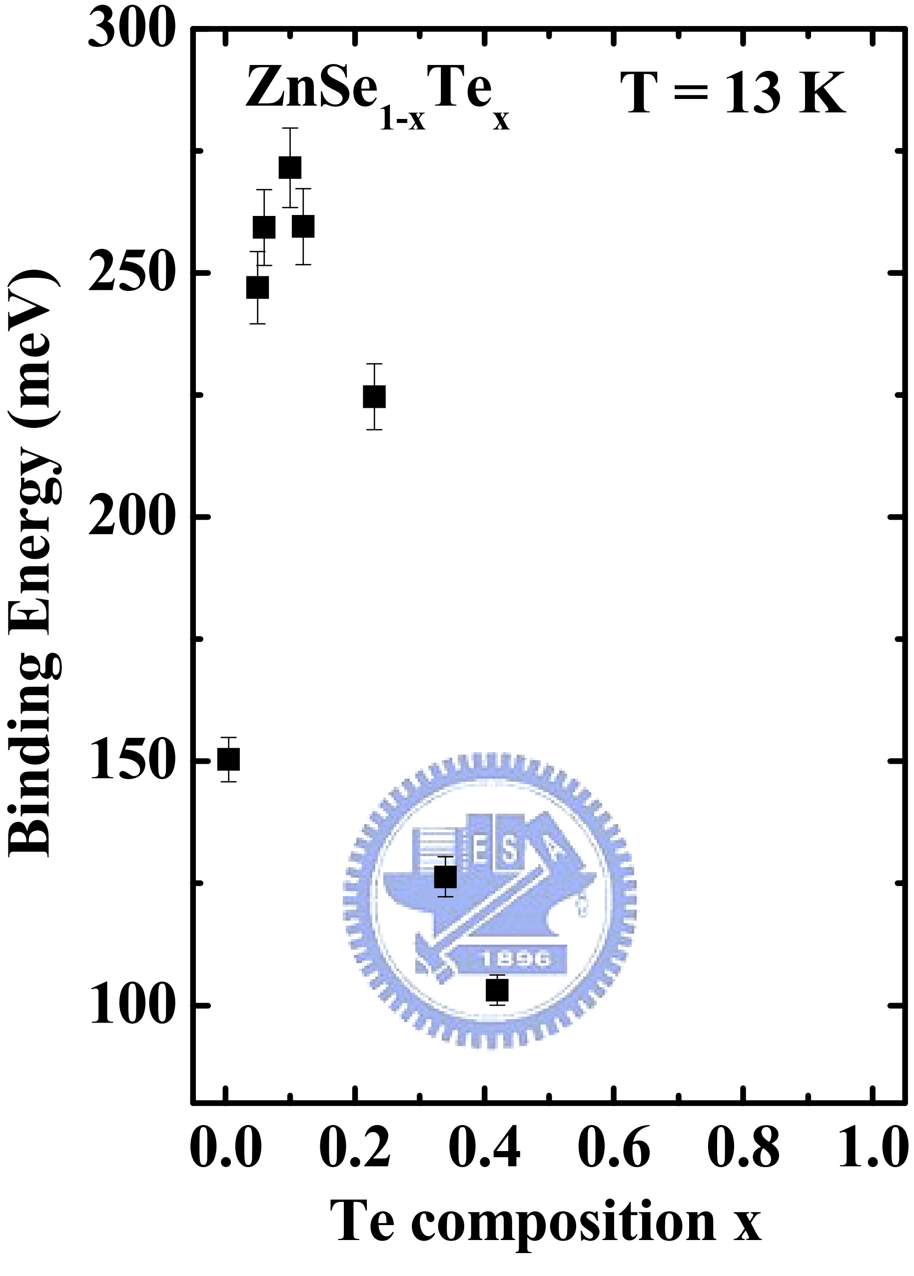

FIG. 3-2. The dependence of exciton binding energy on Te content.

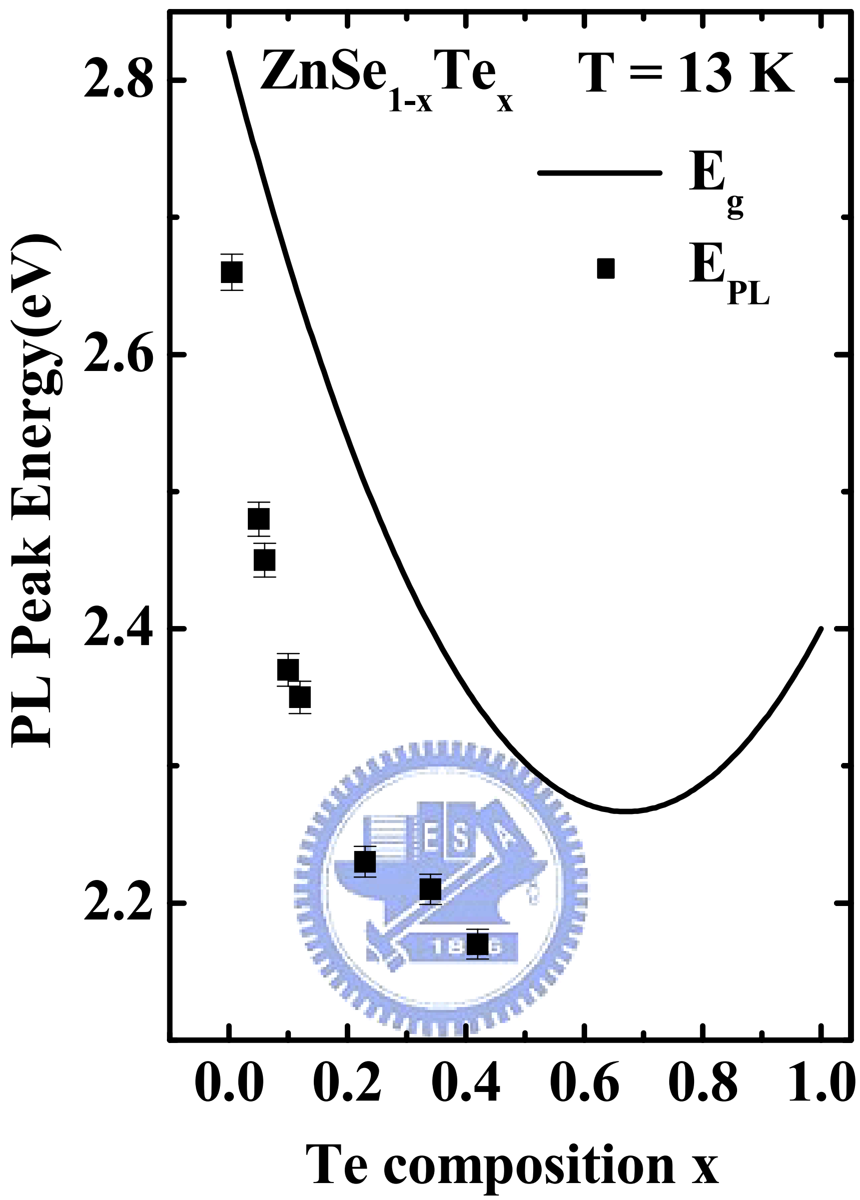

FIG. 3-3. The dependence of the PL peak energy on Te content. The solid curve is band gap energy of $ZnSe_{1-x}Te_x$ at 13 K from Ref. [11].

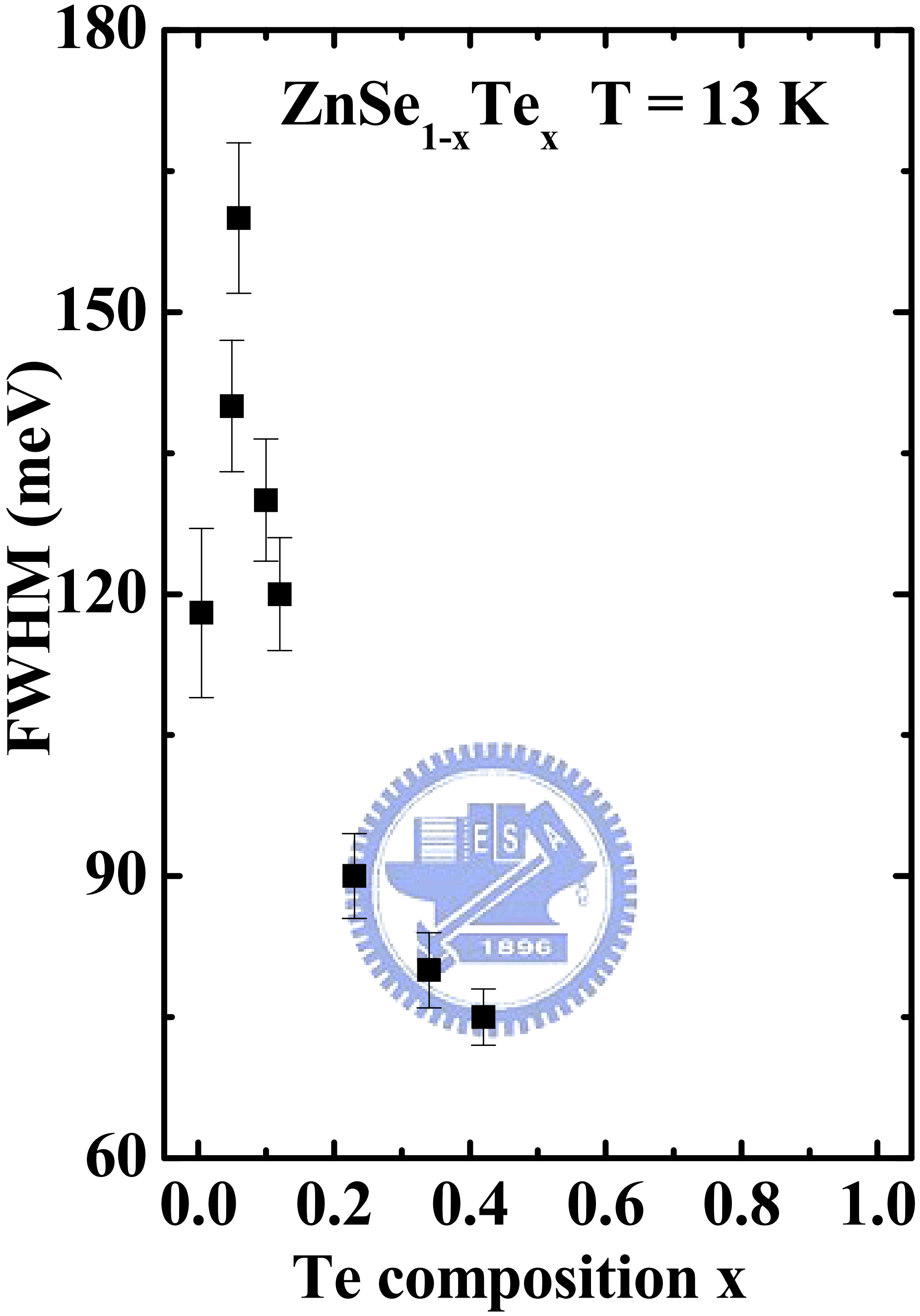

FIG. 3-4. The dependence of FWHM on Te content.

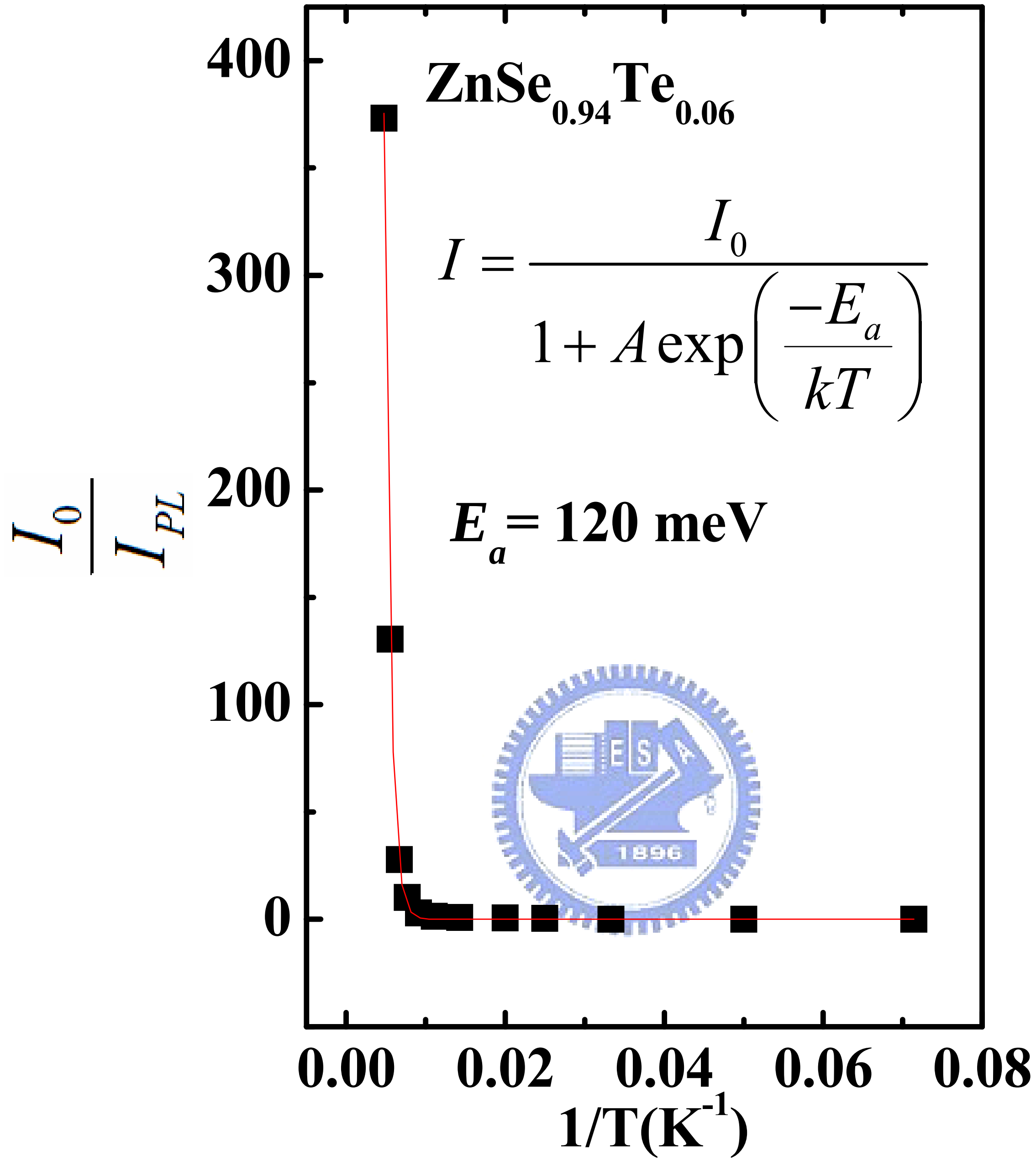

FIG. 3-5. The PL intensity versus temperature of ZnSe$_{0.94}$Te$_{0.06}$ epilayer.

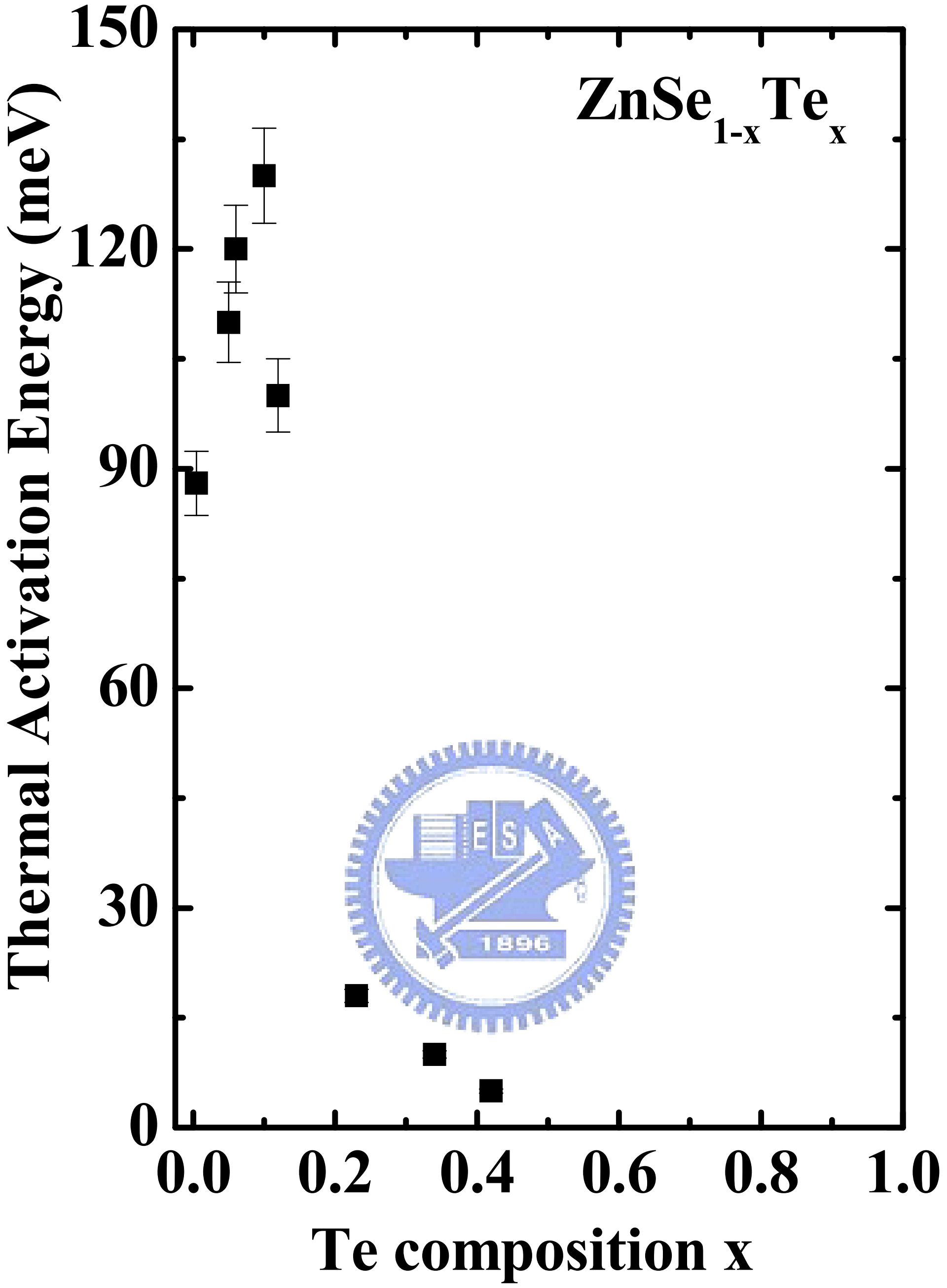

FIG. 3-6. The dependence of thermal activation energy (E_a) on Te content.

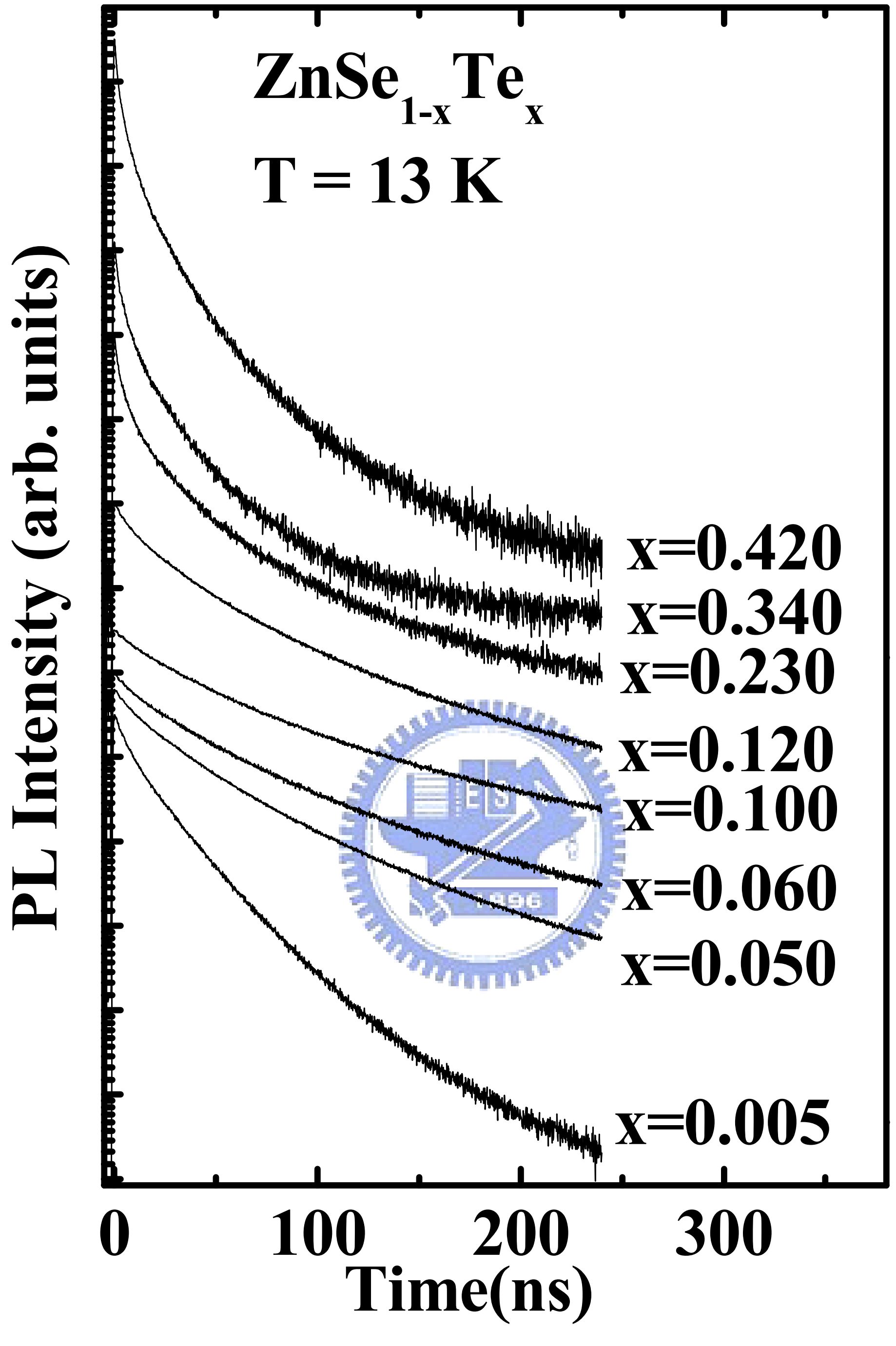

FIG. 3-7. **TRPL spectra of ZnSe$_{1-x}$Te$_x$ (0.005 ≦ x ≦ 0.42) at 13 K.**

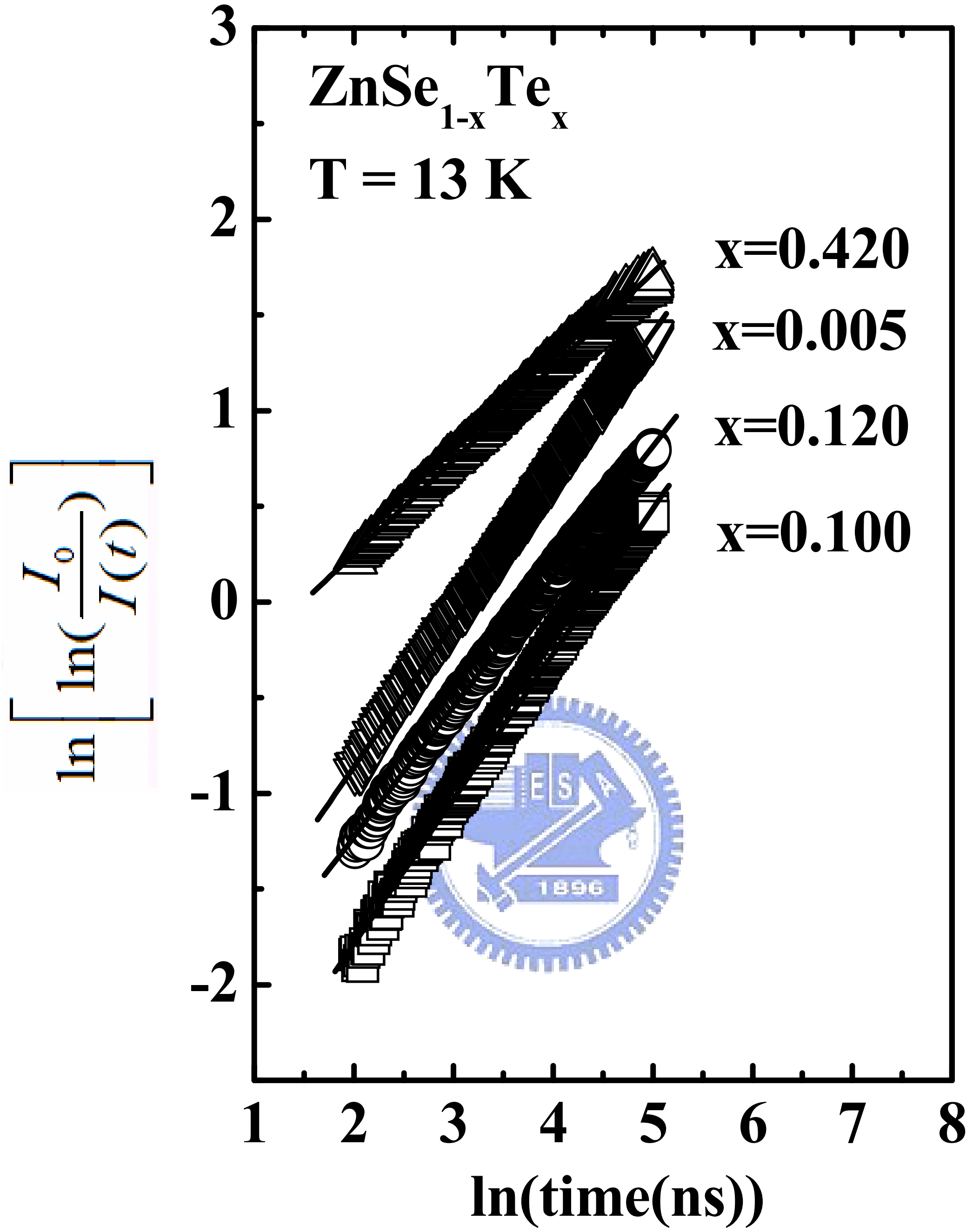

FIG. 3-8.　Stretched exponential of ZnSe$_{1-x}$Te$_x$ ($0.005 \leqq x \leqq 0.42$) at 13 K.

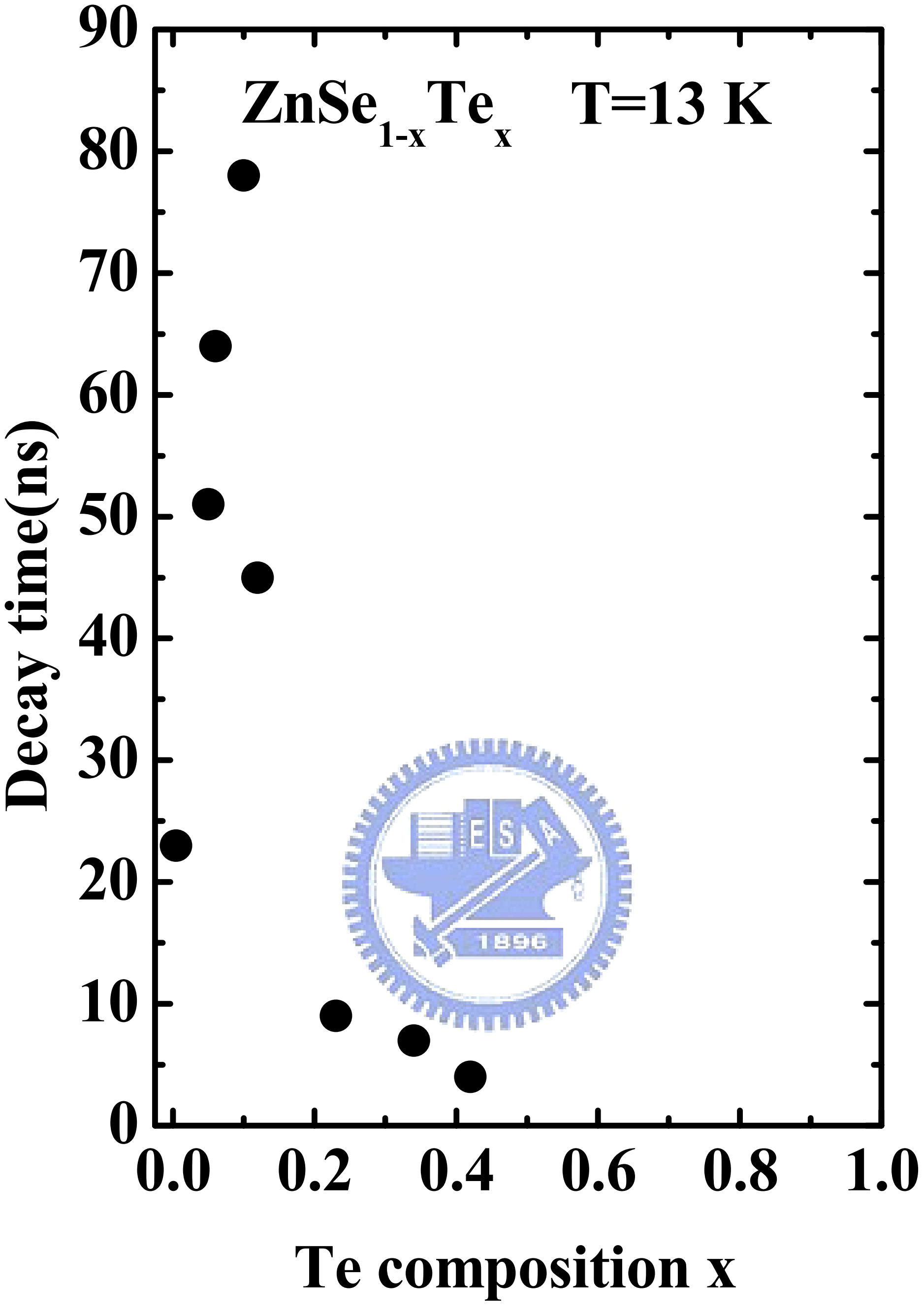

FIG. 3-9. The dependence of PL decay lifetime as a function of x.

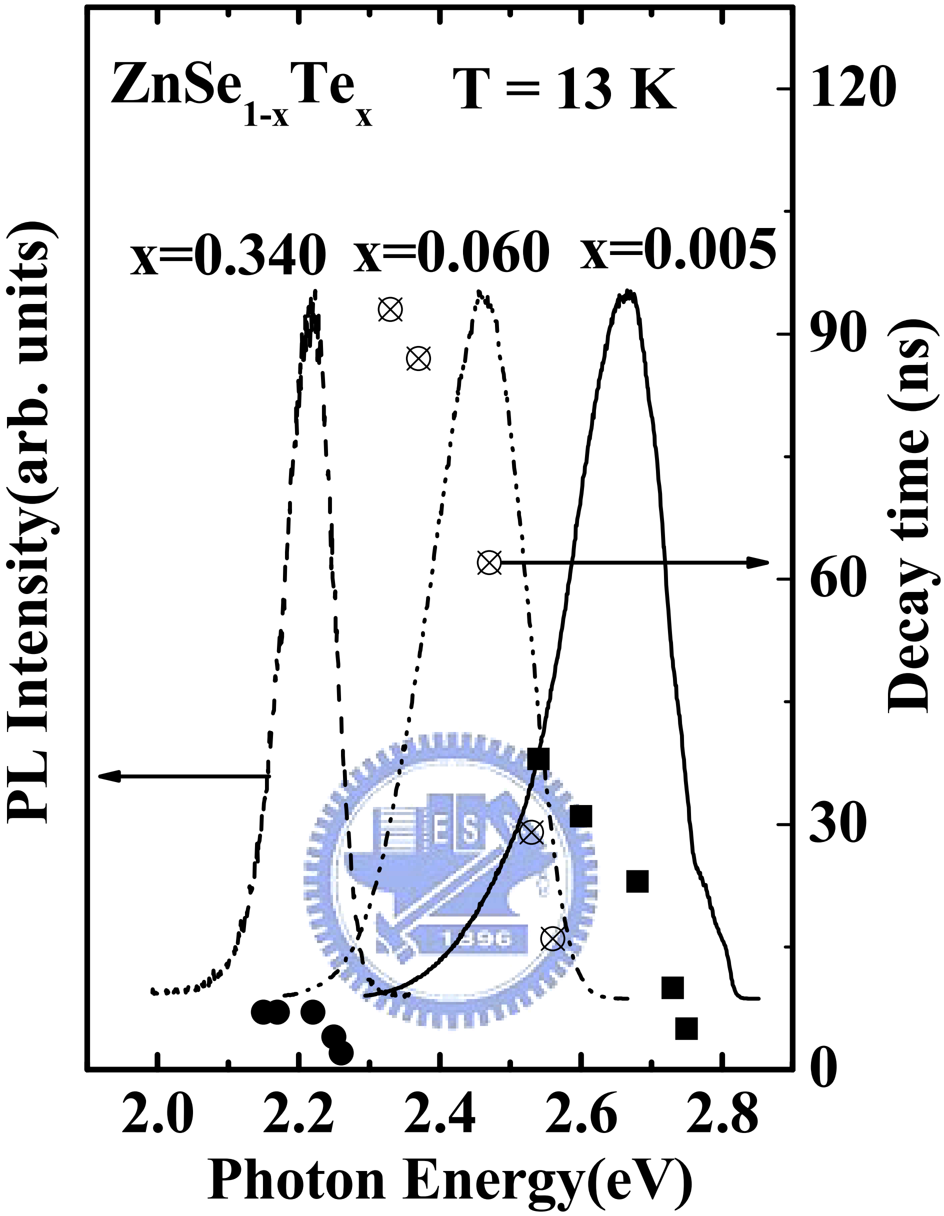

FIG. 3-10. The PL spectra and the decay lifetime as a function of the monitored emission energies for samples with *x*=0.005, 0.060, and 0.340.

Chapter 4: Conclusions

In summary, the decay dynamics of $ZnSe_{1-x}Te_x$ ($0.005 \leqq x \leqq 0.42$) epilayers were investigated by TRPL measurements. The PL lifetime was analyzed by using the stretched exponential function. The recombination lifetime varies from a few nanoseconds to tens of nanosecond with Te concentration. As the Te content increases, the recombination lifetime increases and reaches a maximum at about 78 ns for $x = 0.10$. It is because the more Te content causes larger localization potential. As the Te composition further increases ($x > 0.10$), the recombination lifetime decreases with the increasing of Te concentration. This is due to the fact that the hybridization between the different localize states will be diminishing resulting in the formation of the hybridized states and towards the band state of ZnTe. The decrease of recombination lifetime with x reflects the decreasing percentage of excitons that tunnel between different localize states. This tendency was supported by the dependence of the PL line width, the exciton binding energy, and thermal activation energy on Te concentration.

Reference

[1] C. S. Yang, D. Y. Hong, C. Y. Lin, W. C. Chou, C. S. Ro, W. Y. Uen, W. H. Lan and S. L. Tu, J. Appl. Phys, **83**, 2555 (1998).

[2] P. J. Klar, H. Grüning, W. Heimbrodt, J. Koch, F. Ho¨hnsdorf, W. Stolz, P. M. A. Vicente and J. Camassel, Appl. Phys Lett. **76** 3439 (2000).

[3] Marco Felici, Antonio Polimeni, Mario Capizzi, Y. Nabetani, T. Okuno, K. Aoki, T. Kato, T. Matsumoto, and T. Hirai, Appl. Phys Lett. **88** 101910 (2006).

[4] X. D. Yang, Z. Y. Xu, Z. Sun, B. Q. Sun, I. K. Sou and W. K. Ge, Appl. Phys Lett. **86** 162108 (2005).

[5] D. B. Eason, Z. Yu, W. C. Hughes, W. H. Roland, C. Boney, J. W. Cook, Jr. G. Cantwell and W. C. Harsch, Appl. Phys Lett. **66** 115 (1995).

[6] Igor L. Kuskovsky, C. Tian, G. F. Neumark, J. E. Spanier, Irving P. Herman, W.-C. Lin, S. P. Guo, and M. C. Tamargo, Phys. Rev. B **63**, 155205 (2001).

[7] Qiang Fu, D. Lee, A. V. Nurmikko, L. A. Kolodziejski and R. L. Gunshor, Phys. Rev. B **39**, 3173 (1989).

[8] Reznitsky, S. Permogorov, S. Verbin, A. Naumov, Yu. Korostelin, V. Novozhilov, and S. Prokov'ev, Solid State Commun. 52 13 (1984).

[9] Y. Gu, Igor L. Kuskovsky, M. van der Voort, G. F. Neumark, X. Zhou, and M. C. Tamargo, Phys. Rev. B **71**, 045340 (2005).

[10] Jingbo Li and Lin-Wang Wang, Phys. Rev. B **67**, 205319 (2003).

[11] M. J. S. P. Brasil, R. E. Nahory, F. S. Turco-Sandroff, H. L. Gilchrist, and R. J. Martin, Appl. Phys. Lett. **58**, 2509 (1991).

[12] X. Liu, U. Bindley, Y. Sasaki, and J. K. Furdyna, J. Appl. Phys. **91**, 2859 (2002).

[13] K. B. Nam, J. Li, M. L. Nakarmi, J. Y. Lin, and H. X. Jiang, Appl. Phys. Lett. **84**, 5264 (2004).

[14] Y. T. Shih, W. C. Fan, C. S. Yang, M. C. Kuo, and W. C. Chou, J. Appl. Phys. **94**, 3791 (2003).

[15] Y. T. Shih, Y. L. Tsai, C. T. Yuan, C. Y. Chen, C. S. Yang, and W. C. Chou, J. Appl. Phys. **96**, 7267 (2004).

[16] Naumov, H. Stanzl, K. Wolf, S. Lankes, and W. Gebhardt , J. Appl. Phys. **74**, 6178 (1993).

[17] Lorenzo Pavesi and Matteo Ceschini, Phys. Rev. B **48**, 17625 (1993).

[18] X. Chen, B. Henderson, and K. P. O'Donnell, Appl. Phys Lett. **60,** 2672 (1992).

[19] Lorenzo Pavesi, J. Appl. Phys. **80**, 216 (1996).

[20] M. Pophristic, F. H. Long, C. Tran, I. T. Ferguson, and R. F. Karlicek, Jr., J. Appl. Phys. **86**, 1114 (1999).

[21] M. Dovrat, Y. Goshen, J. Jedrzejewski, I. Balberg, and A. Sa'ar, Phys. Rev. B **69**, 155311 (2004).

[22] M. Cazzanelli and L. Pavesi*, Phys. Rev. B **56**, 15264 (1997).

[23] Germar Schlegel, Jolanta Bohnenberger, Inga Potapova, and Alf Mews, Phys. Rev. Lett. **88**, 137401 (2002).

[24] Satoshi Tanaka, Hideki Koyama, and Nobuyoshi Koshida, Appl. Phys. Lett. **73**, 2334 (1998).

[25] Olivier Labeau, Philippe Tamarat, and Brahim Lounis, Phys. Rev. Lett. **90**, 257404 (2003).

[26] C. D. Lee, H. L. Park, C. H. Chung, and S. K. Chang, Phys. Rev. B. **45**, 4491 (1992).

[27] D. Lee, A. Mysyrowicz, A. V. Nurmikko, and B. J. Fitzpatrick, Phys. Rev. Lett. **58**, 1475 (1987).

[28] J. Wu, W. Walukiewicz, K. M. Yu, J. W. Ager, III, E. E. Haller, I. Miotkowski, A. K. Ramdas, Ching-Hua Su, I. K. Sou, R. C. C. Perera, and J. D. Denlinger, Phys. Rev. B 67, 035207 (2003).